

# D meson mixing as an inverse problem

Hsiang-nan Li,<sup>1</sup> Hiroyuki Umeeda,<sup>1</sup> Fanrong Xu,<sup>2</sup> and Fu-Sheng Yu<sup>3</sup>

<sup>1</sup>*Institute of Physics, Academia Sinica, Taipei, Taiwan 115, Republic of China*

<sup>2</sup>*Department of Physics, Jinan University, Guangzhou 510632, Peoples Republic of China*

<sup>3</sup>*School of Nuclear Science and Technology, Lanzhou University, Lanzhou 730000, Peoples Republic of China*

(Dated: January 14, 2020)

We calculate the parameters  $x$  and  $y$  for the  $D$  meson mixing in the Standard Model by considering a dispersion relation between them. The dispersion relation for a fictitious charm quark of arbitrary mass squared  $s$  is turned into an inverse problem, via which the mixing parameters at low  $s$  are solved with the perturbative inputs  $x(s)$  and  $y(s)$  from large  $s$ . It is shown that nontrivial solutions for  $x$  and  $y$  exist, whose values around the physical charm scale agree with the data in both CP-conserving and CP-violating cases. We then predict the observables  $|q/p| - 1 \approx 2 \times 10^{-4}$  and  $\text{Arg}(q/p) \approx 6 \times 10^{-3}$  degrees associated with the coefficient ratio for the  $D$  meson mixing, which can be confronted with more precise future measurements. Our work represents the first successful attempt to explain the  $D$  meson mixing parameters in the Standard Model.

How to understand the large  $D$  meson mixing in the Standard Model has been a long-standing challenge. All theoretic attempts, including inclusive and exclusive ones, either gave the mixing parameters  $x$  and  $y$  two to three orders lower than the data [1, 2], or cannot explain  $x$  and  $y$  simultaneously [3–5]. This is attributed to the notorious difficulty of charm physics: the charm scale is too heavy to apply the chiral perturbation theory and possibly too light to apply the heavy quark expansion. Moreover, the  $D$  meson mixing, strongly suppressed by the Glashow-Iliopoulos-Maiani (GIM) mechanism [6], is sensitive to nonperturbative SU(3) breaking effects characterized by the strange and down quark mass difference, and to CKM-suppressed diagrams with bottom quarks in the loop. On the contrary, the heavy quark expansion accommodates the data for the  $B_d$  and  $B_s$  meson mixings satisfactorily [7].

In this letter we will analyze the  $D$  meson mixing in a new approach based on a dispersion relation, which relates  $x$  and  $y$  for a fictitious  $D$  meson of an arbitrary mass. The dispersion relation is separated into a low mass piece and a high mass piece, with the former being treated as an unknown, and the latter being input from reliable perturbative results. We then turn the study of the  $D$  meson mixing into an inverse problem: the mixing parameters at low mass are solved as "source distributions", which produce the "potential" observed at high mass. It will be demonstrated by choosing a reasonable strange quark mass that nontrivial solutions for  $x$  and  $y$  exist, whose values around the physical charm quark mass  $m_c \approx 1.3$  GeV match the data in both cases with and without CP violation.

Consider the analytical transition matrix element for a  $D$  meson formed by a fictitious charm quark of invariant mass squared  $s$ ,

$$M_{12}(s) - \frac{i}{2}\Gamma_{12}(s) = \langle D^0(s) | \mathcal{H}_w^{\Delta C=2} | \bar{D}^0(s) \rangle. \quad (1)$$

The effective weak Hamiltonian  $\mathcal{H}_w^{\Delta C=2}$  contains two

four-fermion operators  $(V-A)(V-A)$  and  $(S-P)(S-P)$ , which will be abbreviated to  $V-A$  and  $S-P$  below, respectively. The dispersive part  $M_{12}$  and the absorptive part  $\Gamma_{12}$  obey the dispersion relation [8]

$$M_{12}(s) = \frac{P}{2\pi} \int_0^\infty ds' \frac{\Gamma_{12}(s')}{s-s'}, \quad (2)$$

where  $P$  denotes the principal value prescription. The lower bound of the integration variable  $s'$ , which is of  $O(m_\pi^2)$  with  $m_\pi$  being the pion mass, has been approximated by zero. The diagonalization of the mixing matrix leads to the mass eigenstates  $D_{1,2}$  as linear combinations of the weak eigenstates  $D^0$  and  $\bar{D}^0$ ,  $D_{1,2} = pD^0 \pm q\bar{D}^0$ . The mass and width differences of  $D_{1,2}$  define the mixing parameters

$$x \equiv \frac{m_1 - m_2}{\Gamma} = \frac{2M_{12}}{\Gamma}, \quad y \equiv \frac{\Gamma_1 - \Gamma_2}{2\Gamma} = \frac{\Gamma_{12}}{\Gamma}, \quad (3)$$

in the CP-conserving case with the total decay width  $\Gamma$ .

The elements  $M_{12}$  and  $\Gamma_{12}$  for a heavy meson mixing have been calculated at quark level in leading-order QCD in [9, 10], whose results will be adopted directly below. The  $b$  quark mass  $m_b$  should remain constant in the evaluation of  $\Gamma_{12}$ , so that the fictitious  $D$  meson can decay into a  $b$  quark, as its mass crosses the  $b$  quark threshold. The right hand side of Eq. (2) then contains heavy quark contributions to be consistent with the heavy quark dynamics involved in  $M_{12}$ . The  $V-A$  contribution  $\Gamma_{12}^{V-A}$  is given, for  $s > 4m_b^2$ , by

$$\begin{aligned} \Gamma_{12}^{V-A} \propto & \lambda_s^2 (B_{dd}^{(a)} - 2B_{ds}^{(a)} + B_{ss}^{(a)}) \\ & + 2\lambda_s \lambda_b (B_{dd}^{(a)} - B_{ds}^{(a)} - B_{db}^{(a)} + B_{sb}^{(a)}) \\ & + \lambda_b^2 (B_{dd}^{(a)} - 2B_{db}^{(a)} + B_{bb}^{(a)}), \end{aligned} \quad (4)$$

where  $\lambda_k \equiv V_{ck}V_{uk}^*$ ,  $k = s, b$ , are the products of the Cabibbo-Kobayashi-Maskawa (CKM) matrix elements, and the functions  $B_{ij}^{(a)}$  [10] with the internal quarks  $i, j = d, s, b$  arise from the absorptive contributions of

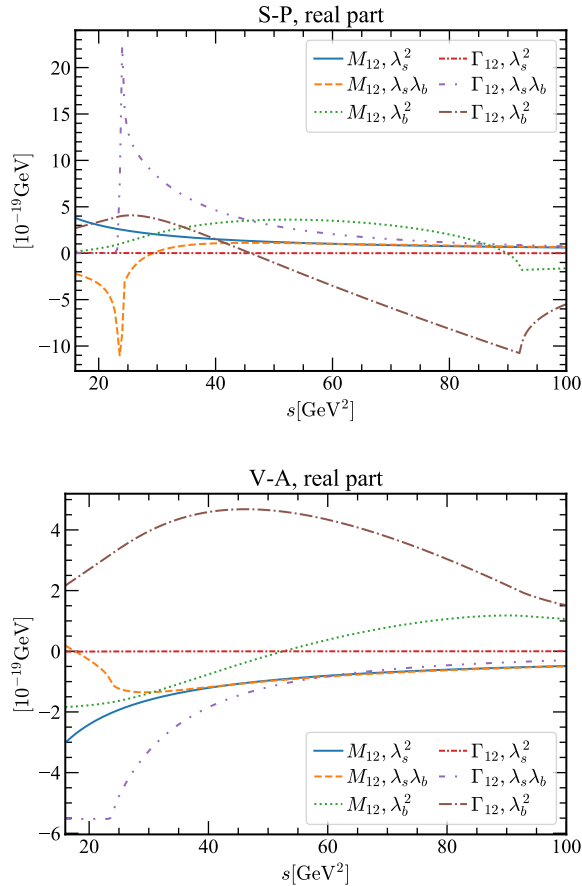


FIG. 1:  $\lambda_s^2$ ,  $\lambda_s \lambda_b$  and  $\lambda_b^2$  contributions to the real parts of  $M_{12}$  and  $\Gamma_{12}$  from the  $S - P$  and  $V - A$  operators.

the box diagrams for Eq. (1). The terms up to  $B_{ss}^{(a)}$  ( $B_{db}^{(a)}$ ,  $B_{sb}^{(a)}$ ) are kept in the range  $s < (m_b + m_d)^2$  ( $(m_b + m_d)^2 < s < (m_b + m_s)^2$ ,  $(m_b + m_s)^2 < s < 4m_b^2$ ). The expression of the  $S - P$  contribution  $\Gamma_{12}^{S-P}$  is similar but with  $B_{ij}^{(a)}$  in Eq. (4) being replaced by  $C_{ij}^{(a)}$  [10]. Equation (4) implies clearly that the  $D$  meson mixing is attributed to the SU(3) symmetry breaking. We have confirmed that  $\Gamma_{12}$  decreases like  $1/s^2$  at large  $s$ , so the integral on the right hand side of Eq. (2) converges.

We rewrite the dispersion relation as

$$\int_0^\Lambda ds' \frac{y(s')}{s-s'} = \pi x(s) - \int_\Lambda^\infty ds' \frac{y(s')}{s-s'} \equiv \omega(s), \quad (5)$$

where both sides have been divided by the measured total width  $\Gamma_{\text{exp}} = 1.61 \times 10^{-12}$  GeV [11] to get the variables  $x$  and  $y$ . The separation scale  $\Lambda$  is arbitrary, but should be large enough to justify the perturbative calculation of  $y$  on the right hand side, and below the  $b$  quark threshold to avoid the  $b$  quark contribution to the left hand side. The product  $f_D^2 m_D$  appearing in the expressions of  $M_{12}$  and  $\Gamma_{12}$  [10] on the right hand side of Eq. (5), with the  $D$  meson decay constant  $f_D$  and its mass  $m_D$ , scales like

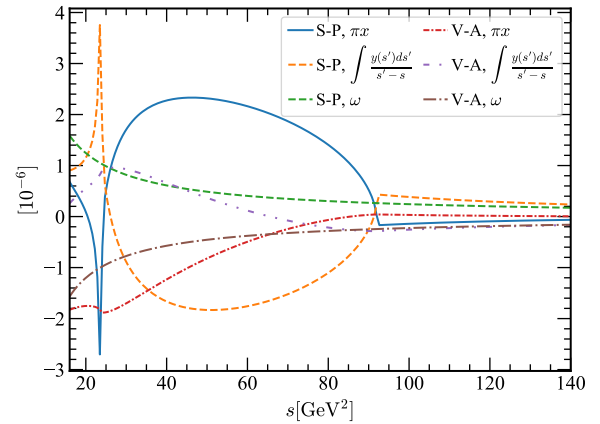
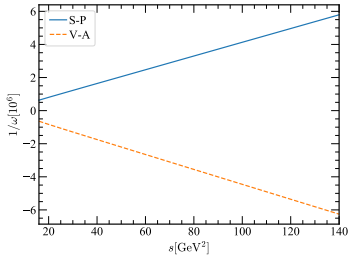


FIG. 2: Dispersive and absorptive contributions to the real part of  $\omega(s)$  from the  $S - P$  and  $V - A$  operators.

a constant in the heavy quark limit. Here we adopt the value for a  $B_s$  meson [11], ie.,  $f_D^2 m_D \sim 0.3$  GeV<sup>3</sup>. The behaviors of  $M_{12}(s)$  and  $\Gamma_{12}(s)$  from the  $S - P$  and  $V - A$  operators with the masses  $m_s = 109.9$  MeV,  $m_b = 4.8$  GeV and  $m_W = 80.379$  GeV, the separation scale  $\Lambda = m_b^2/2 \approx 12$  GeV<sup>2</sup>, and the bag parameters equal to unity are displayed in Fig. 1, which have been decomposed into three pieces proportional to the real parts of  $\lambda_s^2$ ,  $\lambda_s \lambda_b$  and  $\lambda_b^2$ . It is seen in Fig. 2 that both terms on the right-hand side of Eq. (5) exhibit cusps as  $s$  crosses the  $b$  quark and  $b$  quark pair thresholds. However, their sum  $\omega(s)$  behaves smoothly and, furthermore, turns out to be independent of  $m_b$ . This feature, existent for the two four-fermion operators, indicates that  $y$  in the low mass region  $s < \Lambda$  decouples from the  $b$  quark dynamics as expected.

In principle, we can have separate dispersion relations associated with the three CKM products. However, it is reasonable to combine all the terms in Eq. (4) into a single dispersion relation due to the dominance of the  $\lambda_s^2$  contribution to the real part of  $\omega(s)$ . The  $S - P$  and  $V - A$  contributions are opposite in sign, and the corresponding bag parameters are roughly equal. To reduce the sensitivity to the potential cancellation between them, we consider separate dispersion relations for these two operators. Equation (5) will be treated as an inverse problem, in which  $\omega(s)$  for  $s > \Lambda$  from Fig. 2 is an input, and  $y(s)$  in the range  $s < \Lambda$  is solved with the boundary condition  $y(0) = 0$  and the continuity of  $y$  at  $s = \Lambda$ . That is, the "source distribution"  $y(s)$  will be inferred from the "potential"  $\omega(s)$  observed outside the distribution.

For such an ill-posed inverse problem, the ordinary discretization method to solve an integral (Fredholm) equation does not work. The discretized version of Eq. (5) is in the form  $\sum_i A_{ij} y_j = \omega_i$  with  $A_{ij} \propto 1/(i-j)$ . It is easy to find that any two adjacent rows of the matrix  $A$  approach to each other as the grid becomes infinitely fine. Namely,  $A$  tends to be singular, and has no inverse.

FIG. 3:  $s$  dependence of  $1/\omega$ .

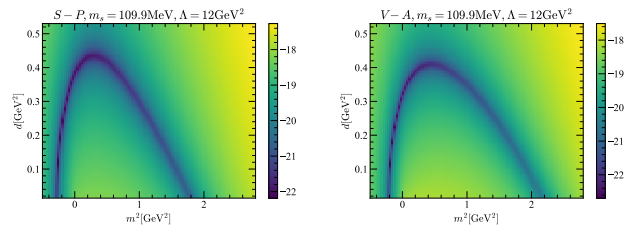
We stress that this singularity, implying no unique solution, should be appreciated actually. If  $A$  is not singular, the solution to Eq. (5) will be unique, which must be the tiny perturbative result obtained in the literature. It is the existence of multiple solutions that allows possibility to explain the observed large  $D$  meson mixing.

We notice that the smooth curves of  $\omega(s)$  can be well described by a simple function  $\omega(s) \propto 1/(s - m^2)$ , as indicated by the almost perfect straight lines for  $1/\omega(s)$  in Fig. 3, with  $m^2 \sim O(1)$  GeV<sup>2</sup>. The power-law behavior is understandable, since only the effect from the monopole component of the distribution dominates at large  $s$ , which decreases like  $1/s$ . The intriguing fact is that the physical charm scale  $m^2 \sim O(m_c^2)$  can emerge from the dispersion relation. If  $\omega(s)$  followed the power law exactly, the solution to Eq. (5) would be a  $\delta$ -function,  $y(s) \propto \delta(s - m^2)$ . The slight deviation from the power-law behavior reflects mild broadening of  $y(s)$  into a sharp peak located at  $s \approx m^2$ . It also justifies that the lower bound of the integration variable in Eq. (5) can be set to zero safely, because  $y(s)$  is supposed to take substantial values only around the charm scale.

Viewing the difficulty to solve an inverse problem, the possible existence of multiple solutions, and the qualitative resonance-like behavior of a solution, we propose the parametrization

$$y(s) = \frac{Ns[b_0 + b_1(s - m^2) + b_2(s - m^2)^2]}{[(s - m^2)^2 + d^2]^2}, \quad (6)$$

and determine the free parameters  $b_0$ ,  $b_1$ ,  $b_2$ ,  $m^2$  and  $d$  from the best fit to the input  $\omega(s)$ . The normalization constant  $N$  is chosen, such that  $Ns/[(s - m^2)^2 + d^2]^2 \rightarrow \delta(s - m^2)$  is respected in the vanishing width limit  $d \rightarrow 0$ . The convergence of the expansion in the numerator will be verified, so keeping terms up to  $(s - m^2)^2$  is enough. It is obvious that Eq. (6) obeys the boundary condition  $y(0) = 0$ . The continuity of  $y(s)$  at  $s = \Lambda$  imposes a constraint among the five parameters. The separation scale  $\Lambda$  introduces an end-point singularity to the integral on the right hand side of Eq. (5), as  $s$  is close to  $\Lambda$ . To reduce the effect caused by this artificial singularity, we consider  $\omega(s)$  from the range  $30 \text{ GeV}^2 < s < 250 \text{ GeV}^2$ , in which 200 points  $s_i$  are selected. For each point  $(m^2, d)$

FIG. 4: Distributions of GOF minima on the  $m^2$ - $d$  plane.

on the  $m^2$ - $d$  plane, we search for  $b_0$  and  $b_1$ , that minimize the deviation

$$\sum_{i=1}^{200} \left| \int_0^\Lambda ds' \frac{y(s')}{s_i - s'} - \omega(s_i) \right|^2. \quad (7)$$

The value of  $b_2$  is derived from the continuity constraint at  $s = \Lambda$ .

The scanning on the  $m^2$ - $d$  plane reveals the arc-shaped distributions of the goodness-of-fit (GOF) minima associated with the  $S - P$  operator shown in Fig. 4. The minima along the arc, having similar GOF, about  $10^{-21}$ - $10^{-22}$  for both operators relative to  $10^{-17}$  from outside the arc, hint that there is no unique solution. As evaluating  $y(s)$  at low  $s$  in perturbation theory, we get different results at various orders, because of the finite running coupling constant  $\alpha_s$  in that region. All these different results lead to almost identical  $\omega(s)$  in the large  $s$  limit, where  $\alpha_s$  diminishes. The solutions from  $m^2$  not close to  $m_c^2$  may correspond to perturbative fixed-order results, since they generate tiny  $y$  at the physical scale  $m_c^2$ , while those near  $m^2 \approx m_c^2$  correspond to nonperturbative results. The observation that they give the same  $\omega(s)$  at large  $s$  realizes the concept of the global quark-hadron duality postulated in QCD sum rules [12]. The arc-shaped distribution from the  $V - A$  operator is also displayed in Fig. 4, where a solution with  $m^2 \approx m_c^2$  has a large  $d$ , so its contribution to  $y$  is negligible.

Selecting a point  $(m^2, d)$  on the arc, we get a solution of  $y(s)$ . Substituting the obtained  $y(s)$  in the whole range of  $s$  into the right hand side of Eq. (2), we calculate the corresponding  $x(s)$ . A solution of  $x(m_c^2)$  and  $y(m_c^2)$  is then compared with the data. It is seen in the upper plot of Fig. 5 that the data  $x = (0.50^{+0.13}_{-0.14})\%$  and  $y = (0.62 \pm 0.07)\%$  in the CP-conserving case [13] can be accommodated simultaneously by the  $S - P$  contribution with the parameters

$$\begin{aligned} m^2 &= 1.713 \text{ GeV}^2, \quad d = 3.876 \times 10^{-2} \text{ GeV}^2, \\ b_0 &= -3.296 \times 10^{-5} \text{ GeV}^2, \quad b_1 = -3.234 \times 10^{-2}, \\ b_2 &= 5.617 \times 10^{-2} \text{ GeV}^{-2}. \end{aligned} \quad (8)$$

To explain the data within  $1\sigma$  errors, the width  $d$  is allowed to vary by 20%. It has been concluded [5] that multi-particle modes in  $D$  meson decays play a crucial role for understanding  $y$ . When  $s$  increases, single

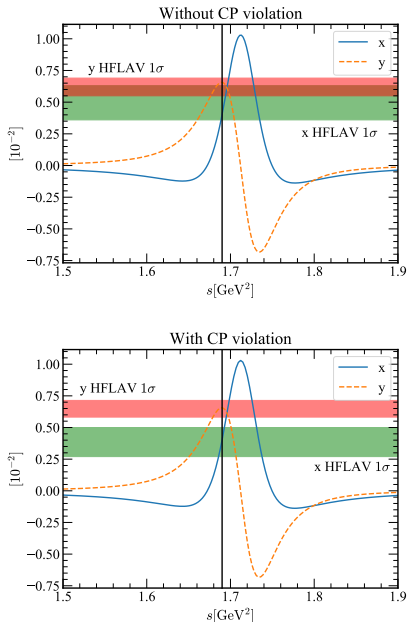


FIG. 5:  $x(s)$  and  $y(s)$  in the cases without and with CP violation. The horizontal bands represent the data with  $1\sigma$  errors, and the vertical lines correspond to  $s = m_c^2$ .

strange quark channels with destructive contributions, like  $KKK\pi$ , are enhanced by phase space, and double strange quark channels with constructive contributions, like  $KKKK$ , are opened. This tendency fits the behavior of  $y(s)$  in Fig. 5, which first decreases from a positive value expected in the two-body analysis [5] to a negative value, and then increases with  $s$ . Hence, the curve in Fig. 5 has caught major features of  $y(s)$ , though its true behavior might be more complicated. We have also examined that the  $b_1$  term dominates, and the  $b_2$  term contributes only about 10% of  $x(m_c^2)$  and  $y(m_c^2)$ . The convergence of the parametrization in Eq. (6) is verified.

As CP violation is allowed, both  $M_{12}$  and  $\Gamma_{12}$  become complex due to the weak phase in the CKM matrix elements, but Eq. (2) still holds. The explicit expressions of  $x$  and  $y$  in terms of the complex  $M_{12}$  and  $\Gamma_{12}$  are referred to [11]. In this case the same parameters  $\Lambda = 12 \text{ GeV}^2$  and  $m_s = 109.9 \text{ MeV}$  are chosen, and the  $\lambda_b^2$  contribution is found to dominate the imaginary part of  $\omega(s)$ . An additional parametrization similar to Eq. (6) but with primed parameters is proposed, and fit to the imaginary part of  $\omega(s)$ . The scanning on the  $m^2$ - $d$  plane yields the arc-shaped distributions of the GOF minima similar to Fig. 4. We find that the parameters in Eq. (8) and

$$\begin{aligned} m'^2 &= m^2 = 1.713 \text{ GeV}^2, & d' &= 4.970 \text{ GeV}^2, \\ b'_0 &= -8.238 \times 10^{-7} \text{ GeV}^2, & b'_1 &= 4.355 \times 10^{-7}, \\ b'_2 &= -7.192 \times 10^{-8} \text{ GeV}^{-2}, \end{aligned} \quad (9)$$

for the  $S-P$  contribution, and those for the  $V-A$  contri-

bution, which are not presented for simplicity, accommodate the data  $x = (0.39_{-0.12}^{+0.11})\%$  and  $y = (0.651_{-0.069}^{+0.063})\%$  [13] simultaneously, as illustrated in the lower plot of Fig. 5. We then derive  $|q/p| - 1 \approx 2 \times 10^{-4}$  and  $\text{Arg}(q/p) \approx (6 \times 10^{-3})^\circ$  associated with the coefficient ratio as predictions, which are comparable to the data  $q/p = (0.969_{-0.045}^{+0.050})e^{i(-3.9_{-4.6}^{+4.5})^\circ}$  [13], and can be confronted with more precise measurements in the future. It is noticed that as  $\Lambda$  increases, say, to  $14 \text{ GeV}^2$ ,  $m_s$  can increase to  $130.6 \text{ MeV}$  accordingly to explain the observed  $x$  and  $y$ . However, our prediction for  $q/p$  is quite stable with respect to the variation of the above parameters. It implies that  $q/p$  can serve as an ideal observable for constraining new physics effects.

This work represents the first successful quantitative attempt to understand the parameters  $x$  and  $y$  for the  $D$  meson mixing in both CP-conserving and CP-violating cases in the Standard Model. The key is to transform the dispersion relation between  $x$  and  $y$  into an inverse problem, in which the nonperturbative observables in the low mass region is solved with the perturbative input from the high mass region. QCD corrections to the  $S-P$  and  $V-A$  operators and to the bag parameters, and high-power corrections can be included in the high mass region systematically to improve the precision of results. Theoretical uncertainties in this approach will be investigated in detail in the future. Once the  $D$  meson mixing parameters are understood, the relevant data, especially those for the coefficient ratio  $q/p$ , can be used to constrain new physics effects appearing in the box diagrams. Extensive applications of our approach are expected.

This work was supported in part by the Ministry of Science and Technology of R.O.C. under Grant No. MOST-107-2119-M-001-035-MY3, and by NSFC under Grant Nos. U1932104 and 11605076.

- 
- [1] E. Golowich and A. A. Petrov, Phys. Lett. B **625**, 53 (2005).
  - [2] M. Bobrowski, A. Lenz, J. Riedl and J. Rohrwild, JHEP **1003**, 009 (2010).
  - [3] H. Y. Cheng and C. W. Chiang, Phys. Rev. D **81**, 114020 (2010).
  - [4] M. Gronau and J. L. Rosner, Phys. Rev. D **86**, 114029 (2012).
  - [5] H. Y. Jiang, F. S. Yu, Q. Qin, H. n. Li and C. D. Lu, Chin. Phys. C **42**, 063101 (2018).
  - [6] S. L. Glashow, J. Iliopoulos and L. Maiani, "Weak Interactions with Lepton-Hadron Symmetry," Phys. Rev. D **2**, 1285 (1970).
  - [7] M. Artuso, G. Borissov and A. Lenz, Rev. Mod. Phys. **88**, 045002 (2016).
  - [8] A. F. Falk, Y. Grossman, Z. Ligeti, Y. Nir and A. A. Petrov, Phys. Rev. D **69**, 114021 (2004).
  - [9] H. Y. Cheng, Phys. Rev. D **26**, 143 (1982).
  - [10] A. J. Buras, W. Slominski and H. Steger, Nucl. Phys.

- B245**, 369 (1984).
- [11] M. Tanabashi et al. (Particle Data Group), Phys. Rev. D 98, 030001 (2018).
- [12] M. A. Shifman, hep-ph/0009131.
- [13] HFLAV Collaboration, <https://hflav.web.cern.ch/>.